

We are IntechOpen, the world's leading publisher of Open Access books Built by scientists, for scientists

6,900

Open access books available

186,000

International authors and editors

200M

Downloads

Our authors are among the

154

Countries delivered to

TOP 1%

most cited scientists

12.2%

Contributors from top 500 universities



WEB OF SCIENCE™

Selection of our books indexed in the Book Citation Index
in Web of Science™ Core Collection (BKCI)

Interested in publishing with us?
Contact book.department@intechopen.com

Numbers displayed above are based on latest data collected.
For more information visit www.intechopen.com



Recrystallization of Dispersion-Strengthened Copper Alloys

Su-Hyeon Kim¹ and Dong Nyung Lee²

¹*Korea Institute of Materials Science,*

²*Seoul National University²*

Republic of Korea

1. Introduction

1.1 Dispersion-strengthened copper alloys

Pure copper exhibits high electrical and thermal conductivities, but it has low strength at room temperature as well as at elevated temperatures. Dispersion-strengthened (DS) copper alloy exhibits a high strength without sacrificing its inherent high conductivities, and maintains excellent thermal and mechanical stability at elevated temperatures by retaining its microstructures (Nadkarni, 1984). These unique characteristics are mainly attributed to the presence of uniformly dispersed thermally stable particles, which are typically oxides. Unlike precipitation-hardened copper alloys, which lose their strength by heating above the initial aging temperatures, the non-metallic oxide particles in oxide DS copper alloys, such as alumina, silica, and beryllia, neither coarsen nor go into solution, effectively preventing recrystallization and consequent softening of the alloys. Alumina DS copper alloys are not recrystallized even after exposure to temperatures approaching the melting point of copper (Preston & Grant, 1961). This is due to the pinning effect of the nano-sized alumina particles on the movement of the boundaries and dislocations. A unique combination of high strengths and high conductivities at elevated temperatures makes alumina DS copper alloys good candidates for high temperature electric materials (e.g., electrodes, lead wires, and connectors) (Nadkarni, 1984) as well as potential components in nuclear energy applications (Sumino et al., 2009).

Alumina DS copper alloys can be recrystallized when boron is added (Kim & Lee, 2001, 2002). Boron is often intentionally added as an oxygen scavenger during fabrication of the alloys (Gallagher et al., 1992). Long term annealing of boron-added alumina DS copper alloys results in an unexpected transformation from fine γ -Al₂O₃ to coarse 9Al₂O₃-2B₂O₃ with a concurrent recrystallization of the matrix to form a large and elongated grain structure (Kim & Lee, 2002). Whereas Ni-based DS alloys are used in a coarse-grained condition to increase high-temperature creep resistance (Gessinger, 1976; Stephens & Nix, 1985), key applications of alumina DS copper alloys require them to be in a fully work-hardened state. Consequently, a large decrease in room temperature strength due to recrystallization is not desirable. Therefore, an understanding of the recrystallization behaviour of DS copper alloys is important from both practical and theoretical perspectives.

1.2 Recrystallization of particle-containing alloys

The presence of dispersed particles critically affects the plastic deformation and recrystallization behaviour of the matrix. The presence of particles accelerates or retards recrystallization of the matrix, depending on the interparticle spacing, size, mechanical properties, and thermal stability of the particles (Humphreys & Hatherly, 1995). Closely spaced fine particles exert a pinning effect on the movement of boundaries (Zener drag) resulting in retardation or even complete suppression of recrystallization. However, alloys with widely spaced particles larger than $\sim 1 \mu\text{m}$ show accelerated recrystallization. Non-deformable large particles can introduce deformation zones around the particles during deformation, providing favourable nucleation sites for recrystallization (particle stimulated nucleation, PSN). Under certain conditions, particle-containing alloys transform from a deformed structure to a recrystallized grain structure in the absence of conventional discontinuous recrystallization accompanying a long-range motion of the boundaries. During low-temperature annealing, small particles give rise to boundary pinning, and subsequent coarsening of the particles at high temperatures may allow the subgrains to grow, forming recrystallized grain structures. This phenomenon is sometimes known as continuous recrystallization.

1.3 Purpose of the study

While several studies exist on the fabrication methods, mechanical properties, and deformation behaviour of alumina DS copper alloys, there is a lack of understanding of their recrystallization behaviour. This study examines the recrystallization behaviour of boron-added alumina DS copper strips rolled under different conditions. Particular attention is given to several anomalous phenomena, such as unique recrystallized grain structures and textures, as well as the dependency of recrystallization characteristics on prior rolling conditions. The results of several microscopy studies to elucidate microstructural evolution during rolling and annealing are presented, and the effects of dispersed particles on recrystallization are examined.

2. Research methods

2.1 Materials

The material used in this study was commercially available alumina DS copper alloy strips, Glidcop Al25, produced by SCM Metal Products. This material contains 0.25wt% Al in the form of Al_2O_3 particles as well as 0.02wt% B used for oxygen scavenging. The thickness of the as-received strips was $840 \mu\text{m}$. The chemical composition of the as-received strips was measured by inductively coupled plasma (ICP) analysis and given in Table 1.

Al	B	P	Fe	S	As	Mn	Cu
0.275	0.023	0.0001	0.0001	0.0001	0.0034	0.0001	Balance

Table 1. Chemical composition of the as-received strips measured by ICP (wt%)

2.2 Rolling and annealing

The as-received strips were rolled under lubrication using a two-high rolling mill whose roll diameter was 126 mm to make two different specimens, as listed in Table 2. The cold-rolled strips were further rolled to reduce their thickness by 25% with one pass at room temperature. The thickness of the hot-rolled strips was reduced by 27% with one pass after heating the strips at 813 K for 10 minutes. Isothermal annealing of the as-received and rolled strips was carried out in a salt bath. After the heating, the strips were quenched in water.

Specimen	Number of passes	Total reduction	Rolling temperature	Lubrication
Cold-rolled strip	1	25%	Ambient	Yes
Hot-rolled strip	1	27%	813 K	Yes

Table 2. Rolling conditions of the as-received strips

2.3 Microstructure and texture analysis

The microstructures of the strips were investigated by optical microscopy and transmission electron microscopy (TEM) in the transverse direction (TD) and the normal direction (ND). The specimens were cut from the strips, mechanically polished, and chemically etched in FeCl_3 solution prior to optical microscopy. For the TEM study, the specimens were electrically polished in a nitric acid solution to make a thin foil using a twin-jet electro-polisher, while the dispersed alumina particles were extracted from the material using a carbon replica method.

The macroscopic textures of the strips were determined by measuring (111), (200), and (220) pole figures with an X-ray diffraction goniometer in the back reflection mode with $\text{Co K}\alpha$ radiation. The specimens were mechanically polished parallel to the rolling plane and chemically etched in a nitric acid solution. Three-dimensional orientation distribution functions (ODFs), complete pole figures, and orientation densities were calculated from the measured pole figures using the WIMV program (Matthies et al., 1987). The orientations of individual crystallites were calculated from the Kikuchi patterns obtained by TEM (Young, et al. 1973) in the TD section of the specimens. Misorientations between adjacent crystallites were calculated using 24 symmetry operations (Randle, 1993).

2.4 Analysis of the mechanical properties

Tensile tests of specimens with a gauge length of 30 mm along the rolling direction (RD) were carried out at room temperature at a crosshead speed of 1 mm/min. The micro-Vickers hardness of the specimens was measured under a load of 25 g for 10 s.

3. Results

3.1 Characterization of the as-received strips

Figure 1 shows the microstructures of the as-received strips observed under an optical microscope. The material exhibited a highly deformed microstructure consisting of fine band-like substructures aligned nearly parallel to the RD. Figure 2 shows the longitudinal

section TEM microstructure observed in the surface and centre regions of the as-received strips. The average band thicknesses of the surface and the centre regions were 0.127 and 0.129 μm , respectively. Additional band boundary characteristics measured on the centre region are given in Table 3. The grain structure of the as-received strips was characterized by a fine band-like grain structure with a high-angle boundary character.

The mechanical properties of the as-received strips are given in Table 4. The high strengths and hardness indicate that the strips were heavily deformed.

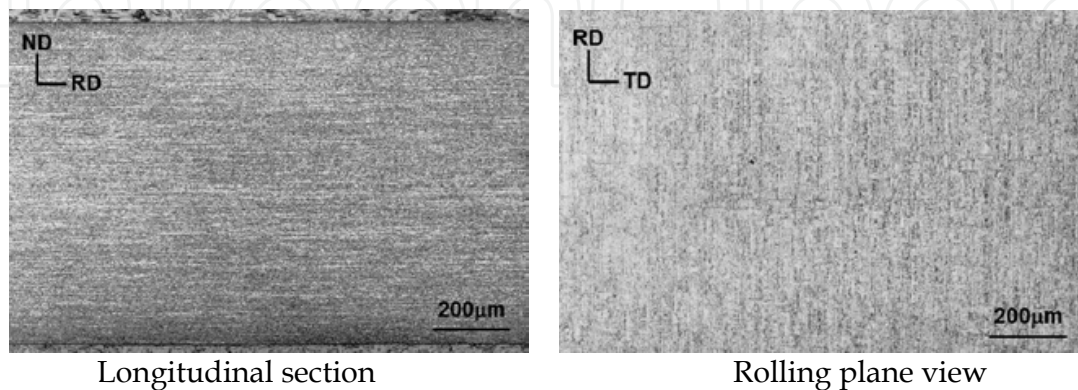


Fig. 1. Optical micrographs of the as-received strips

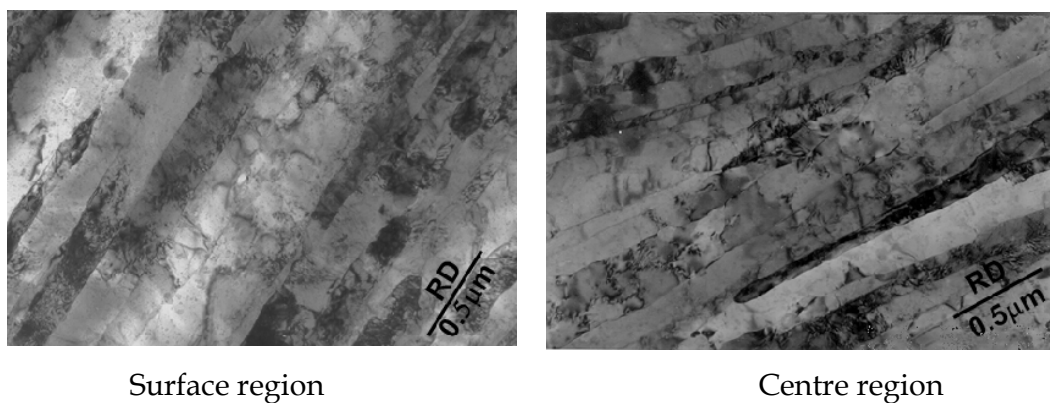


Fig. 2. Longitudinal section TEM micrographs of the as-received strips

Specimen	Average band thickness (μm)	Average boundary misorientation (deg)	High angle boundary fraction (misorientation ≥ 15 deg)
As-Received	0.129	30.6	0.52

Table 3. Band boundary characteristics of the as-received strips

Specimen	Tensile strength (MPa)	Yield strength (MPa)	Elongation (%)	Hardness (Hv)
As-Received	553	515	14	169

Table 4. Mechanical properties of the as-received strips

Figure 3 shows the texture evolution of the as-received strips. The texture was characterized by the β -fibre, running from the copper orientation $\{112\}\langle 111 \rangle$ over the S orientation $\{123\}\langle 634 \rangle$ to the brass orientation $\{011\}\langle 211 \rangle$ in the Euler orientation space. The well-developed β -fibre texture indicated that the received strip was in a heavily rolled state, which is consistent with the microstructure evolution shown in Figures 1 and 2. Figure 4 shows the orientation densities along the β -fibre of the surface and the centre regions. The orientation densities of the brass and the S components were higher than the copper component, which is unlike plane-strain rolled pure copper sheets where the copper component is dominant (Hirsch & Lücke, 1988). Also noteworthy is the fact that the density of the brass component was lower than that of the S component in the surface region, while the brass and the S components were almost equally dominant in the centre region.

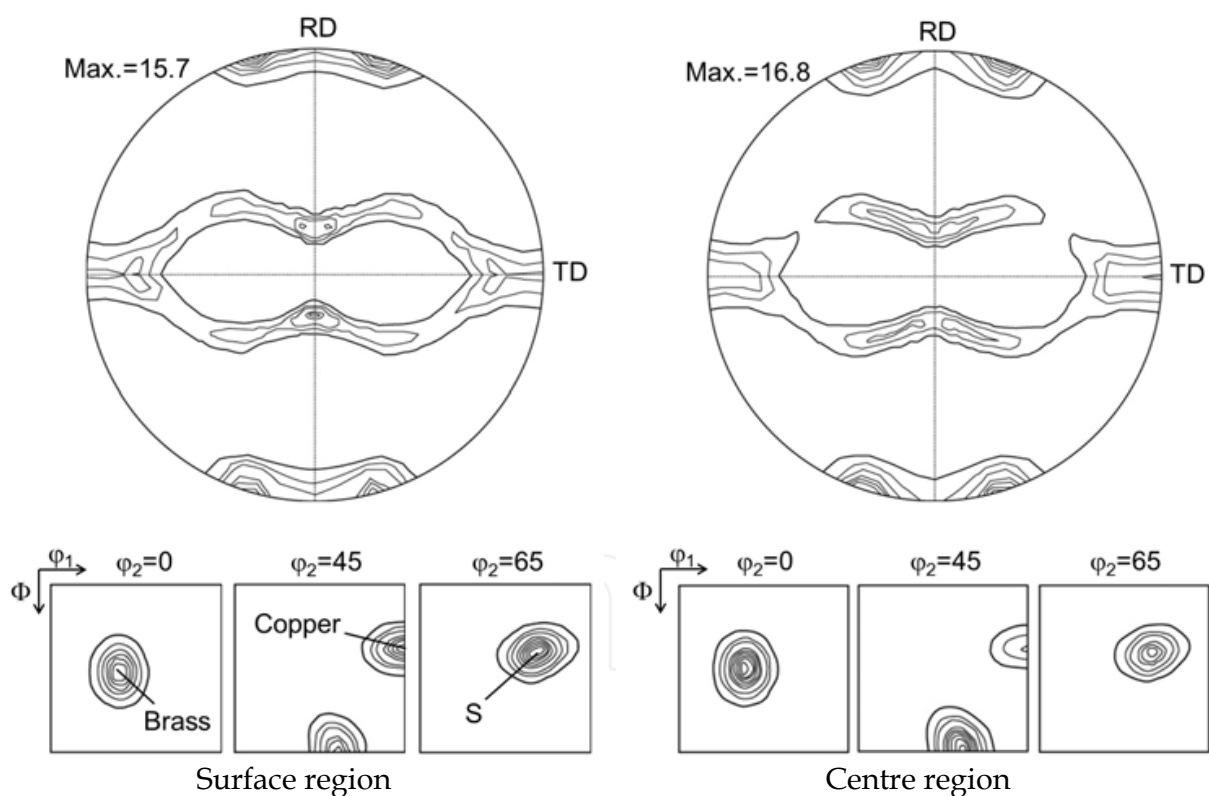


Fig. 3. (111) pole figures and ODFs of the surface and the centre layers of the as-received strips (Kim & Lee, 2002)

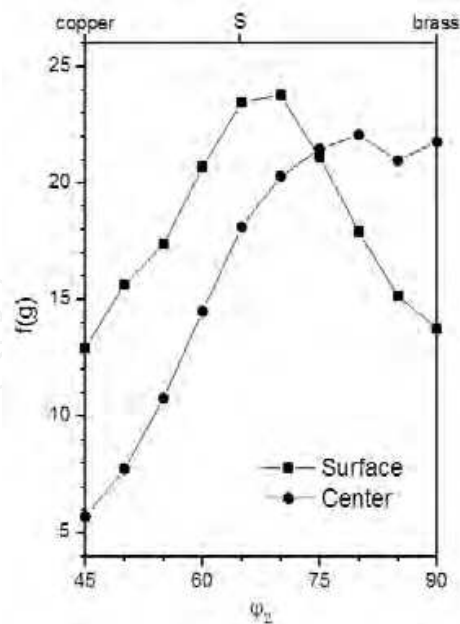


Fig. 4. Orientation densities along the β -fibre of the surface and the centre regions of as-received strips

Figure 5 shows optical microstructures of the as-received strips annealed at 1123 K for 1 hr. Recrystallization occurred in the centre region while no recrystallization took place in the surface region. The plate-like morphology of the recrystallized grains and the ragged shape of the grain boundaries are similar to other extruded or rolled dispersion-strengthened alloys after recrystallization (Klug et al., 1996; Chou, 1997). The TEM microstructures of a recrystallized grain (Figure 6) show dispersed particles aligned parallel to the rolling direction in the recrystallized regions. The micro-Vickers hardness values of the centre and the surface regions were 136 and 168, respectively. This result indirectly indicates that the centre region was recrystallized but the surface region was not. Figure 7 shows the TEM plane view observation of a recrystallized grain in the centre region. A large plate-like recrystallized grain was identified. The textures of the annealed strips are visible in Figure 8. The surface region retained the β -fibre texture, which was similar to the texture in the rolled state. The centre region exhibited a strong texture component, which could be approximated by $\{112\}\langle 312\rangle$. The texture of the centre region originated from the recrystallized grains.

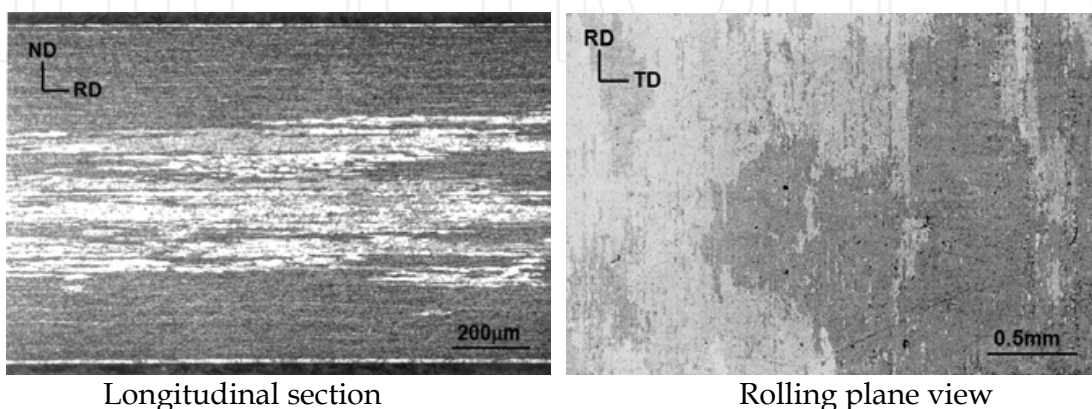


Fig. 5. Optical micrographs of the as-received strips annealed at 1123 K for 1 hr

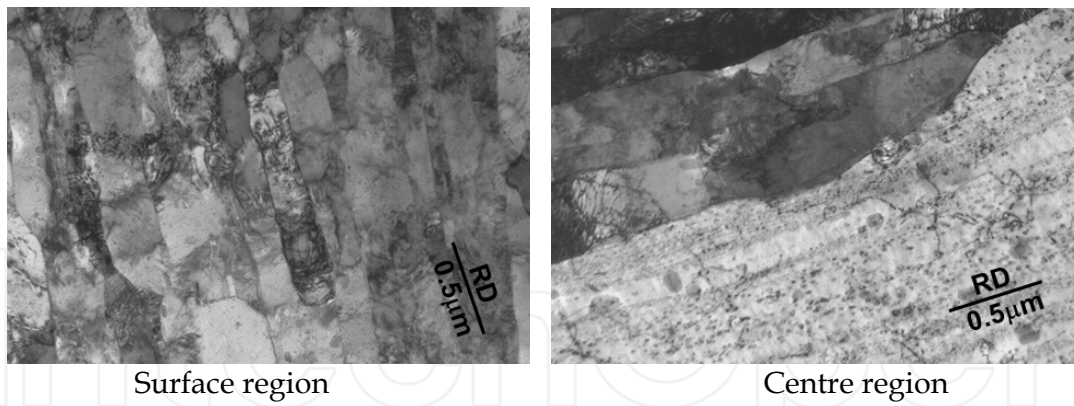


Fig. 6. Longitudinal section TEM micrographs of the as-received strips annealed at 1123 K for 1 hr

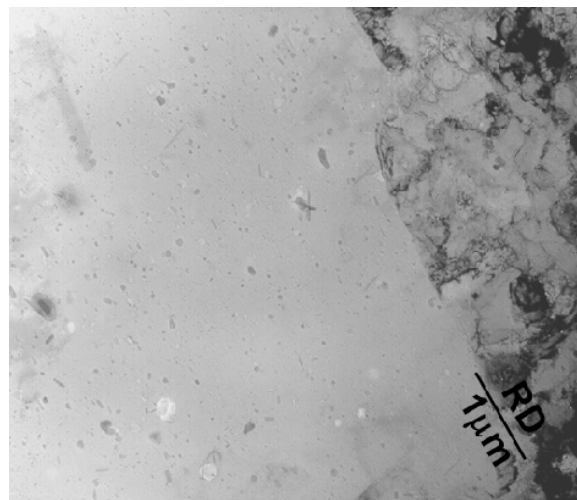


Fig. 7. Rolling plane view TEM micrographs of the centre region of the as-received strips annealed at 1123 K for 1 hr

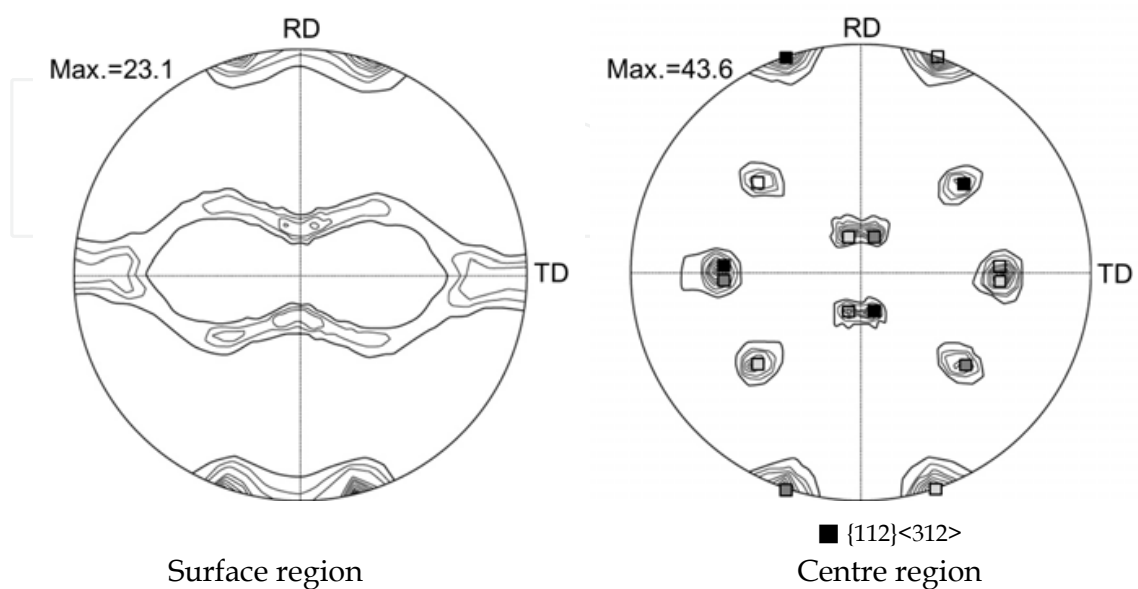


Fig. 8. (111) pole figures of the as-received strips annealed at 1123 K for 1 hr (Kim & Lee, 2002)

3.2 Properties of the rolled strips

Figures 9 and 10 show optical and TEM microstructures of the cold-rolled and hot-rolled strips. Band-like structures aligned parallel to the RD were observed that were similar to those of the as-received strips. No dynamically recrystallized grains were found in the hot-rolled strips. Table 5 details the band structure characteristics of the cold-rolled and hot-rolled strips measured in the centre regions of each strip. By comparing the band structure characteristic of the as-received strips given in Table 3, the thickness of the band was decreased by cold rolling and increased by hot rolling. Cold rolling also increased the high-angle boundary fraction.

Table 6 shows the mechanical properties of the rolled strips. The cold-rolled strip showed higher strengths and hardness than the hot-rolled strip. By comparing the properties to those of the as-received strips, it can be seen that both cold rolling and hot rolling increased the strengths and hardness of the strips while decreasing their elongation.

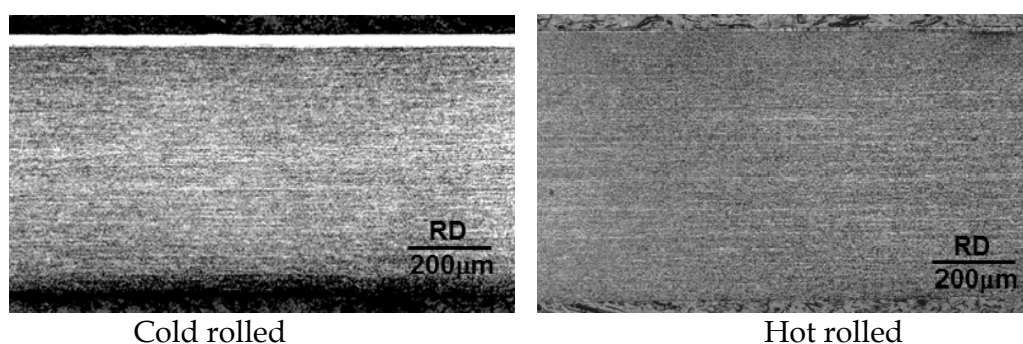


Fig. 9. Longitudinal section optical micrographs of the rolled strips (Kim & Lee, 2002)

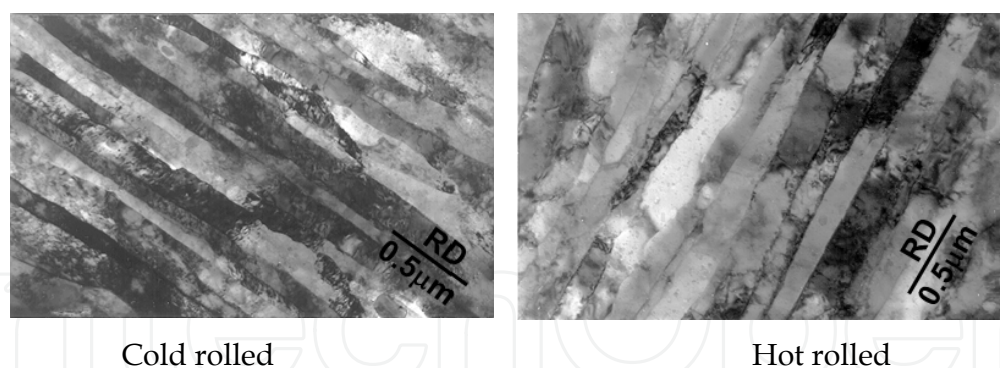


Fig. 10. Longitudinal section TEM micrographs of the centre region of the rolled strips (Kim & Lee, 2002)

Specimen	Average band thickness (μm)	Average boundary misorientation (deg)	High angle boundary fraction (misorientation ≥ 15 deg)
Cold rolled	0.116	27.9	0.60
Hot rolled	0.141	24.5	0.51

Table 5. Band structure characteristics of the cold-rolled and hot-rolled strips

Specimen	Tensile strength (MPa)	Yield strength (MPa)	Elongation (%)	Hardness (Hv)
Cold rolled	605	579	5	184
Hot rolled	580	553	5.5	179

Table 6. Mechanical properties and hardness of the cold-rolled and hot-rolled strips

The textures of the rolled strips were similar to those of the as-received strips. Figure 11 shows the orientation densities along the β -fibre of the surface and the centre regions of the rolled strips. The textures of the rolled strips were characterized by the strong β -fibre.

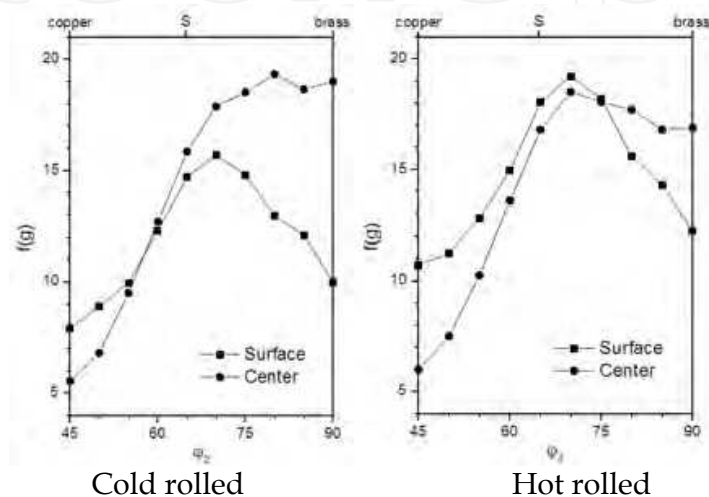


Fig. 11. Orientation densities along the β -fibre of the surface and centre regions of the rolled strips

Figure 12 shows the optical microstructures of the rolled strips annealed at 1123 K for 1 hr. TEM micrographs of the centre region are given in Figure 13. Similar to the as-received strips, the cold-rolled strips exhibited recrystallization in the centre region while the hot-rolled strips did not show recrystallization since no recrystallized grains were observed throughout the examined area. However, substantial band growth appeared on the hot-rolled strip. Table 7 gives the band structure characteristics of the hot-rolled and annealed strips. By comparing the results in Tables 5 and 7, it appears that annealing increased the band thickness and high-angle boundary fraction of the hot-rolled strip.

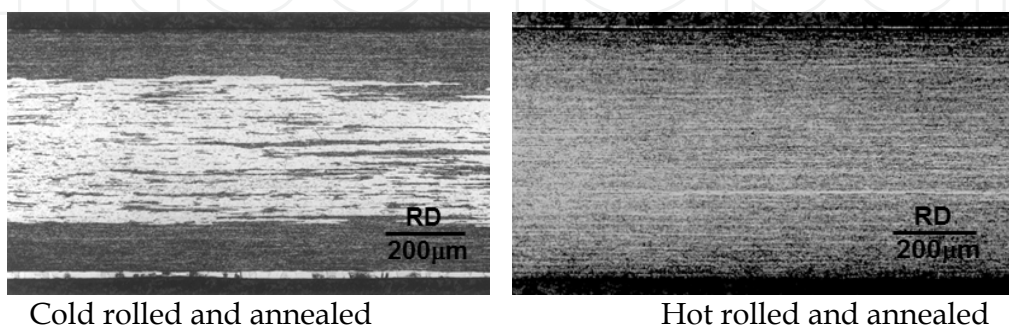


Fig. 12. Longitudinal section optical micrographs of the rolled strips annealed at 1123 K for 1 hr (Kim & Lee, 2002)

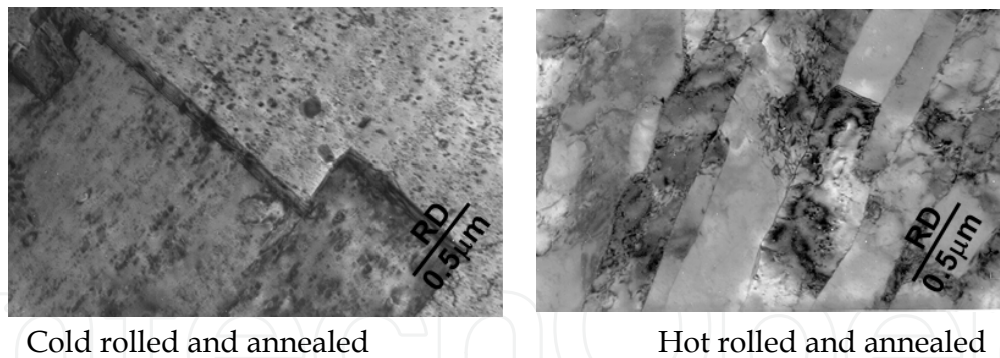


Fig. 13. Longitudinal section TEM micrographs of the centre region of the rolled strips annealed at 1123 K for 1 hr (Kim & Lee, 2002)

Specimen	Average band thickness (μm)	Average boundary misorientation (deg)	High angle boundary fraction (misorientation ≥ 15 deg)
Hot rolled and annealed	0.270	36.0	0.81

Table 7. Band structure characteristics of the hot-rolled strip annealed at 1123 K for 1 hr

Figure 14 shows (111) pole figures of the cold-rolled strip annealed at 1123 K for 1 hr. The texture of the surface region was characterized by the β -fibre, and the recrystallization texture in the centre region was indexed by $\{112\}\langle 312 \rangle$. The texture of the hot-rolled strip after annealing is shown in Figure 15. Both the surface and the centre regions retained most of the β -fibre rolling texture.

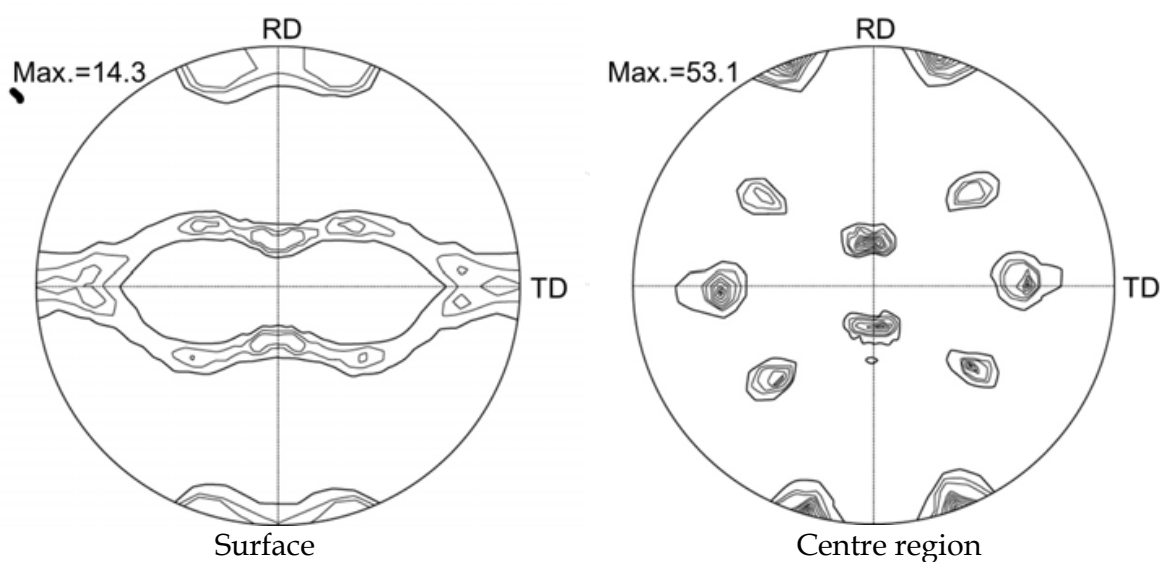


Fig. 14. (111) pole figures of the cold-rolled strip annealed at 1123 K for 1 hr (Kim & Lee, 2002)

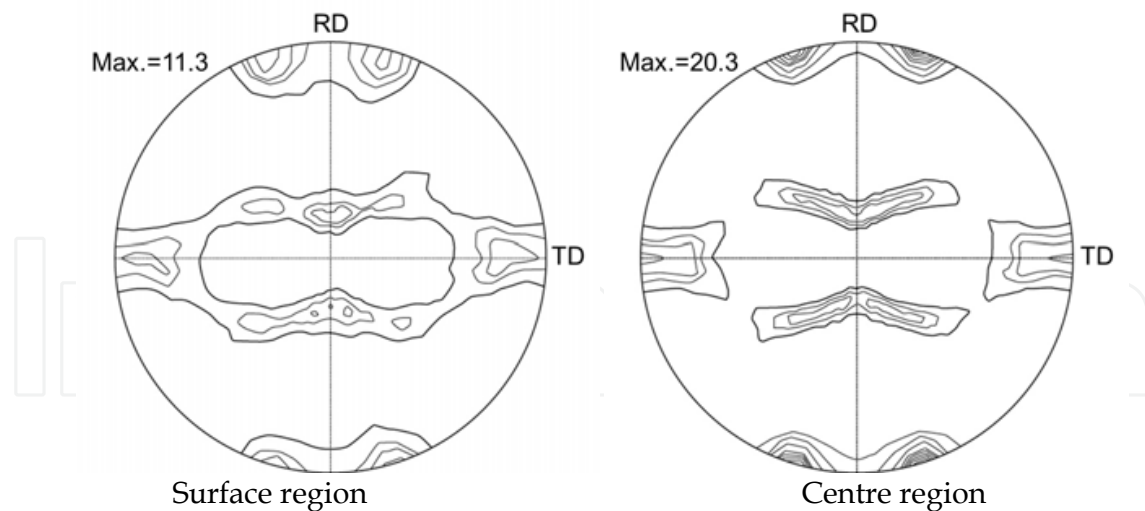


Fig. 15. (111) pole figures of the hot-rolled strip annealed at 1123 K for 1 hr (Kim & Lee, 2002)

4. Discussion

Earlier studies (Preston & Grant, 1961; Nadkarni, 1984) have shown that alumina DS copper alloys resist recrystallization up to their melting points due to the presence of thermally stable alumina particles. The present study showed that alumina DS copper alloys recrystallized after moderate-temperature annealing when boron was added. This is attributed to a reduction in the particle-pinning effect caused by the transformation of particles from fine alumina to coarse aluminium boron oxide. Additionally, large particles already present in the deformed state can introduce deformation zones that act as nucleation sites for recrystallization. Alumina DS copper alloys are fabricated by internal oxidation of Cu–Al alloy powders, consolidations of the powders into fully dense shapes, and further cold rolling to final shapes. The internal oxidation involves the mixing and heating of the alloy powders with oxidants like Cu_2O . Frequently, residual oxygen, or unconverted Cu_2O , may react with hydrogen introduced during alloy processing. This produces a large internal pressure of water vapour and results in blister formations. The material used in this study, Glidcop, is made oxygen-free by intentionally adding boron as an oxygen scavenger. Figure 16 shows a coarse particle observed in the as-received strips, which was identified as $9\text{Al}_2\text{O}_3\text{-}2\text{B}_2\text{O}_3$ by indexing its diffraction patterns. Phase transformation of the particles is expected during the fabrication of a strip since it is subjected to a heating process.

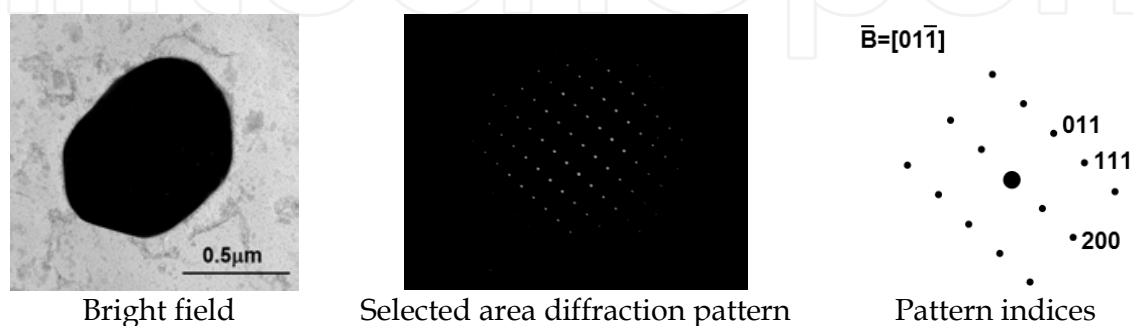


Fig. 16. Identification of an existing large particle observed in the as-received strip (Kim & Lee, 2002)

The remainder of the discussion explores several anomalous phenomena observed during the annealing of the alumina DS copper alloy.

4.1 Unique recrystallized microstructure

The recrystallized microstructure of the boron-added alumina DS copper alloy strip was characterized by the following features:

- Recrystallization only in the centre region
- Plate-like morphology of recrystallized grains
- Very large recrystallized grains

Figures 5 and 12 show that recrystallization occurred only in the centre region of the strips. In order to observe how the microstructure evolved, both the as-received strips and the cold-rolled strips were quickly annealed. Figure 17 shows optical micrographs of the as-received strip annealed at 923 K for 10 s and 15 min. Recrystallized grains emerged along lines originating exclusively from the centre region. Detailed TEM observations revealed that large bands were present in the deformed state in the centre region and appeared to promote recrystallization. Figure 18 shows a large band found in the centre region of the as-received strip, along with its orientation. Figure 19 reveals that similar bands were present in the cold-rolled strips. The orientations of the large bands in the as-received and cold-rolled strips included cube, RD-rotated cube, copper, and ND-rotated copper. Among them, the ND-rotated copper orientation was similar to the recrystallization texture $\{112\}\langle 312 \rangle$ observed in the annealed strips. These pre-existing large bands survived the early stages of annealing as shown in Figures 20 and 21.

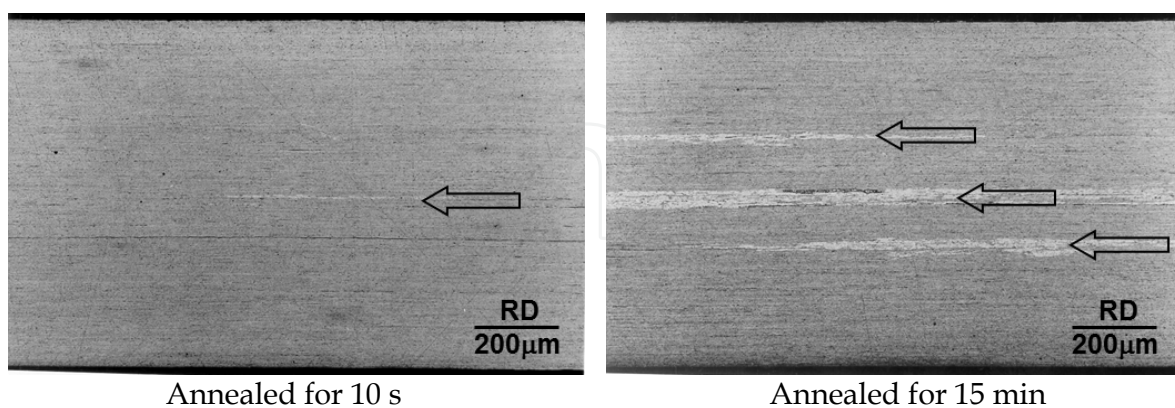


Fig. 17. Longitudinal section optical micrographs of the strips annealed at 923 K

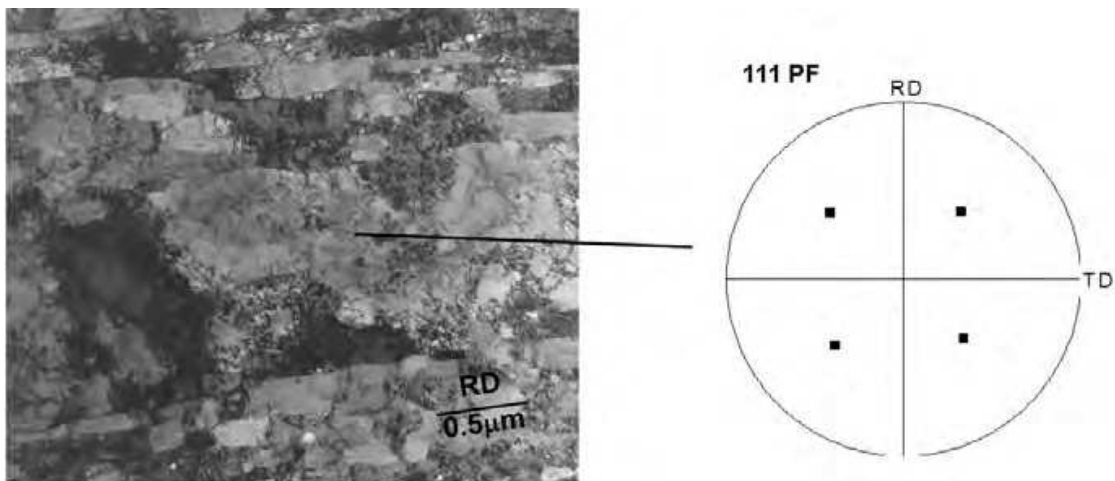


Fig. 18. Longitudinal section TEM micrograph showing a large band and its orientation in the centre region of the as-received strip (Kim & Lee, 2002)

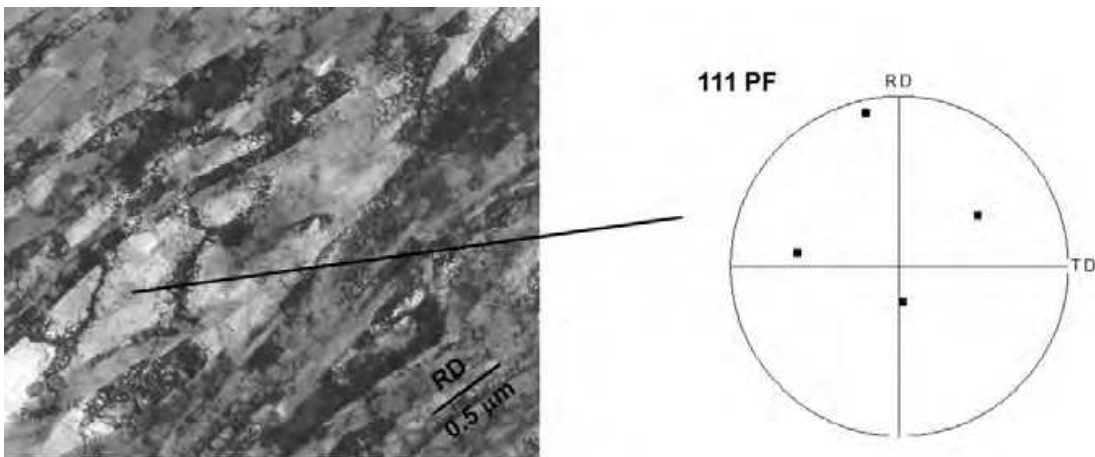


Fig. 19. Longitudinal section TEM micrograph showing a large band and its orientation in the centre region of the cold-rolled strip (Kim & Lee, 2002)

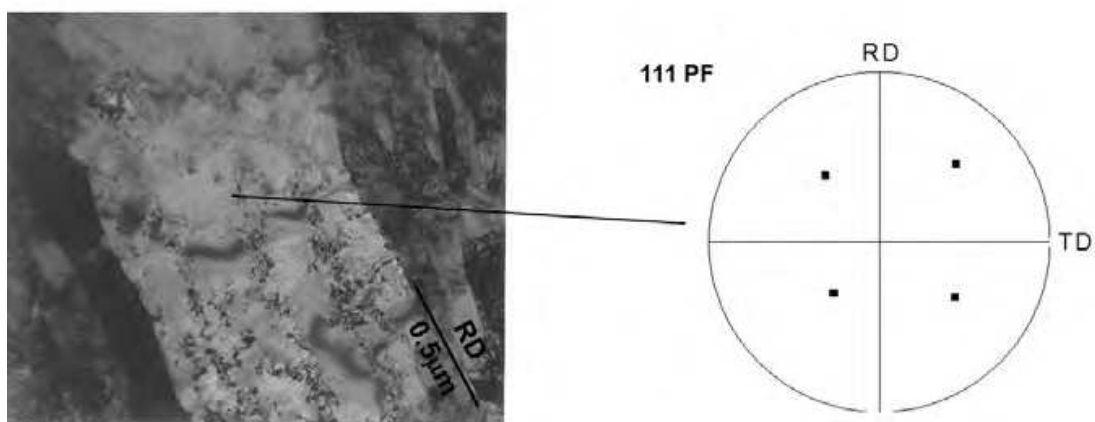


Fig. 20. Longitudinal section TEM micrograph showing a large band and its orientation in the centre region of the as-received strip annealed at 1123 K for 1 s

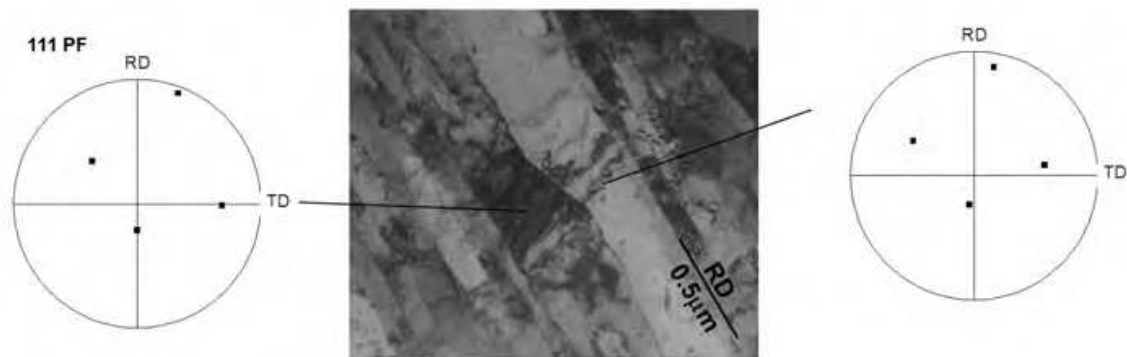


Fig. 21. Longitudinal section TEM micrograph showing a large band and its orientation in the centre region of the cold-rolled strip annealed at 1123 K for 1 s

Recrystallization can be divided into two consecutive processes: nucleation and growth. A nucleus must be some minimum size in order for further growth to occur, or else it will shrink and vanish. Subgrain coalescence is a requisite process to form these critical-sized nuclei. Band coalescence in the present material is unlikely when the band boundaries exhibit high-angle characteristics and their movement is hindered by the presence of dispersed particles. A more likely explanation is that the pre-existing large bands provide favourable nucleation sites for recrystallization. It appears that the large bands present in the centre region are the preferred recrystallization nucleation sites. It is possible that the large bands originated from large grains formed during the manufacturing process as similar grains have been observed in extruded alumina DS copper alloys in previous studies (Afshar & A. Simchi, 2008; H. Simchi & A. Simchi, 2009).

The plate-like morphology of the recrystallized grains in the alumina DS copper alloys can be related to the distribution of the dispersed particles. When recrystallized grains grow, the moving boundaries are pinned by the particles. The pinning pressure of the particles on the boundary movement is given by Equation 1 (Humphreys & Hatherly, 1995):

$$P_Z = 3F_V \gamma_b / d \quad (1)$$

where:

F_V is the volume fraction of the particles

d is the particle size

γ_b is the boundary energy

If particles are randomly distributed, the pinning pressure will be directionally isotropic. On the other hand, if the distribution of the particles is anisotropic, there will be an anisotropic pinning pressure on the boundaries. Figure 5 shows that the particles in the as-received strips were aligned along the rolling direction. The pinning pressure parallel to the rolling plane should be lower than that along the thickness direction. Therefore, the plate-like recrystallized grain shape can be mainly attributed to the planar distribution of the particles. The directional distribution of the particles might be driven by the rolling of the strip. A plate-like morphology of the recrystallized grains is often reported in the recrystallization behaviour of other dispersion-strengthened alloys (Klug et al., 1996; Chou, 1997), although other dispersion-strengthened alloys show equiaxed recrystallized grain structures (Miodownik et al., 1994; Miodownik et al., 1995).

Another unique recrystallization characteristic of the alumina DS copper alloy is that the recrystallized grains are very large. Early researchers (Singer & Gessinger, 1982; Mino et al., 1987; Kusunoki et al., 1990) reported that the very large recrystallized grains found in dispersion-strengthened alloys are formed through secondary recrystallization. They concluded that primary recrystallization occurred immediately before secondary recrystallization, or during plastic deformation – dynamic recrystallization. Later studies (Klug et al., 1996) suggested that primary recrystallization was responsible for the formation of large grains because microstructural changes are driven by stored energy acquired from plastic deformation. While plastically deformed alumina DS copper alloy possesses a sufficient driving force for recrystallization, a barrier to recrystallization exists due to the particle pinning effect. Microstructural inhomogeneity, such as large bands, provides preferential nucleation sites, and a large nucleus at a large band can grow with a size advantage over the surrounding matrix. Therefore, the emergence of very large recrystallized grains is a result of preferential nucleation at pre-existing large bands. The annealing behaviour of alumina DS copper alloy might be regarded as secondary recrystallization since very large recrystallized grains are formed when they overcome the particle-pinning pressure. However, the microstructure of the alumina DS copper alloy suggests that the driving force for recrystallization is stored energy by plastic deformation. Thus, while the evolution of the annealed alumina DS copper alloy microstructure appears to be due to secondary recrystallization, the mechanism that forms the very large recrystallized grains is due to primary recrystallization.

4.2 Unique recrystallization texture

The recrystallization texture of the annealed alumina DS copper alloy can be approximated by $\{112\}\langle 312 \rangle$. To our knowledge, this texture has not been reported for other copper alloys. The recrystallization texture is determined by the orientations of the new grains and their growth rates. The present study discussed the role of these two factors and how they determine the unique recrystallization texture of the alumina DS copper alloy.

4.2.1 Selective nucleation

As discussed previously, pre-existing large bands provided favourable nucleation sites for recrystallization. Pre-existing large particles could introduce particle deformation zones that act as nucleation sites. Figure 22 shows the recrystallizing grains formed around the particles and their orientations observed in the as-received strips after rapid annealing. The orientation of grain A was similar to that of the deformed matrix, and multiple twinning could cause grains B and C to generate different orientations. It is known that PSN usually gives rise to weak recrystallization textures (Humphreys & Hatherly, 1995). Band coalescence is unlikely but possible when the pinning of the boundary movement is relaxed. Figure 23 shows that the band growth took place by coalescence of similarly oriented bands. Various orientations could be generated from new grains resembling the matrix orientations through PSN and band coalescence, as well as by subsequent twinning. Since no specific grain orientations dominated as the new grains evolved, the well-developed strong recrystallization texture $\{112\}\langle 312 \rangle$ could not be caused by new grain evolution.

4.2.2 Selective growth

According to the theory of selective growth, the recrystallization texture is determined by the relative growth rates of the boundaries. The velocity of the moving boundary (V) is a function of the boundary mobility (M) and the driving pressure (P), given by:

$$V=MP \quad (2)$$

P can be expressed as follows:

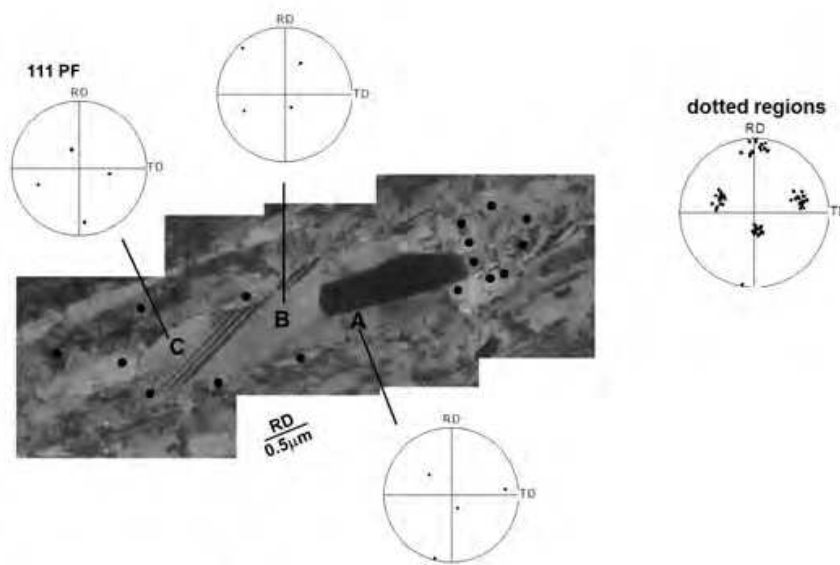


Fig. 22. Longitudinal section TEM micrograph showing individual grains around a particle and their orientations in the as-received strips annealed at 923 K for 10 s

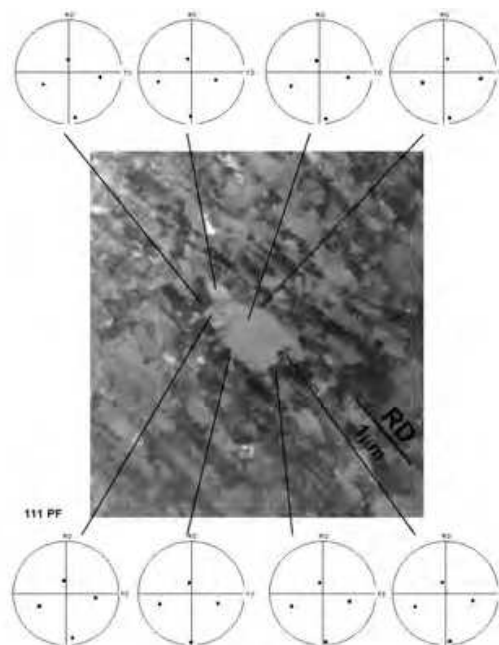


Fig. 23. Longitudinal section TEM micrograph showing individual grains and their orientations in the cold-rolled strips annealed at 1123 K for 3 s (Kim & Lee, 2002)

$$P = P_D - P_C = P_D - 2\gamma_b / R \quad (3)$$

where:

P_D is the stored energy,

P_C is the opposing pressure from the boundary curvature

γ_b is the boundary energy

R is the radius of the grain.

In particle-strengthened alloys, the Zener pinning pressure (P_Z) arises from the particles, and P can be expressed as follows (Humphreys & Hatherly, 1995):

$$P = P_D - P_C - P_Z = P_D - 2\gamma_b / R - 3F_V \gamma_b / d \quad (4)$$

where:

F_V is the volume fraction of the particles

d is the particle size.

Recrystallizing grains will grow only when P is positive. P increases with increasing grain size and decreasing boundary energy. The low-angle boundaries and twin boundaries have a lower boundary energy than the high-angle boundaries. Based on Equation 4, only large grains with low-angle boundaries or twin boundaries can overcome the pinning pressure. High-angle boundaries can be stagnant, even though they have higher mobility than low-angle boundaries. The recrystallization texture $\{112\}\langle 312 \rangle$ is defined as ND-rotated copper, which is occasionally found in large bands in the deformed state, as shown in Figures 19 and 21. Recrystallizing grains with $\{112\}\langle 312 \rangle$ orientations have a chance to face the surrounding deformed matrix with low-angle boundaries because $\{112\}\langle 312 \rangle$ orientations deviate slightly from the deformation texture. Furthermore, $\{112\}\langle 312 \rangle$ orientations have a twinning relationship between the two equivalent orientations among them. Figure 24 shows the orientations of two adjacent recrystallized grains observed in the cold-rolled and annealed strips. The boundary shape and orientation relationship indicated that the grain boundary of the two adjacent recrystallized grains was a twin boundary. Therefore, the unique recrystallization texture was determined by the preferential growth of large recrystallizing grains with low-angle boundaries or twin boundaries, even though those boundaries had low mobility.

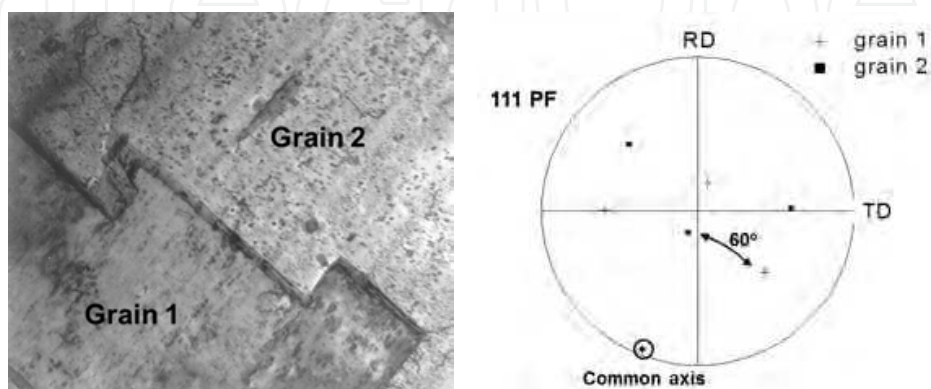


Fig. 24. Longitudinal section TEM micrograph and (111) pole figure showing two adjacent recrystallized grains of the cold-rolled strips annealed at 1123 K for 1 hr

4.3 Dependency of recrystallization on prior rolling conditions

As described in Section 3.2, the response to annealing of the alumina DS copper alloy is influenced by prior rolling conditions. The annealing behaviour of the cold-rolled strip is characterized by recrystallization, whereas recovery by band growth occurs in the hot-rolled strip. Similar results have been reported for other dispersion-strengthened alloys (Petrovic & Ebert, 1972; Singer & Gessinger, 1982). As recovery and recrystallization are competitive processes, dynamic recovery during hot rolling could reduce the potential energy in the alloy. This argument would also apply when comparing results between the cold-rolled and hot-rolled strips; since the hardness of the hot-rolled strip is lower, the recovery process during hot-rolling is governed by normal band growth. In our tests, after annealing, a continuous band growth occurred in the hot-rolled strip, which became a coarse band structure with high-angle boundary characteristics (see Table 7).

Subjecting the as-received strips to hot rolling gave rise to band growth and increased the hardness. Plastic deformation during hot rolling could increase the dislocation density, increasing the hardness. Therefore, a reduction in potential energy may not occur during hot rolling. It is not clear at this time why the hot-rolled strips became resistant to recrystallization. One explanation would be the homogeneity of the microstructural evolution. Microstructural inhomogeneity often occurs during plastic deformation, and these regions are frequently sites of initial recrystallization. The deformation becomes more homogeneous as the deformation temperature increases (Humphreys & Hatherly, 1995). A reduction in microstructural inhomogeneity during hot rolling could be responsible for the suppression of discontinuous recrystallization.

An alternative explanation is based on the assumption that coarse particles are sheared into finer particles during hot rolling (Kim & Lee, 2002). The shear strength of the particle might decrease with increasing temperature. Particle shearing could result in a decrease in interparticle spacing, which in turn could give rise to the higher hardness and the corresponding difficulty in recrystallization.

5. Conclusions

The recrystallization behaviour of boron-added alumina DS copper alloy strips was studied. The results may be summarized as follows.

Recrystallization occurred only in the centre region of the strips. Pre-existing large bands provided a favourable nucleation site for very large recrystallized grains.

The morphology of the recrystallized grains was plate-like due to the planar alignment of the dispersed particles.

The recrystallization texture was indexed to $\{112\}\langle 312\rangle$. Preferential growth of the large recrystallizing grains against the particle pinning appeared to determine this unique recrystallization texture.

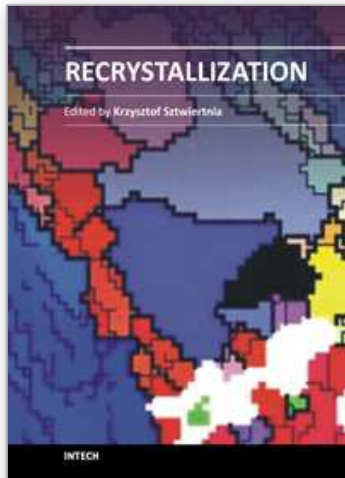
The hot-rolled strip underwent recovery accompanied by continuous band growth, but without recrystallization.

6. References

- Afshar, A. & Simchi, A. (2008). Abnormal Grain Growth in Alumina Dispersion-Strengthened Copper Produced by An Internal Oxidation Process. *Scripta Materialia*, Vol.58, No.11, (June 2008), pp.966-969, ISSN 1359-6462
- Chou, T.S. (1997). Recrystallization Behavior and Grain Structure in Mechanically Alloyed Oxide Dispersion Strengthened MA956 Steel. *Materials Science and Engineering A*, Vol.223, No.1-2, (February 1997), pp. 78-90, ISSN 0921-5093
- Gallagher, D.E.; Hoyt, E.W. & Kirby, R.E. (1988). Surface Segregation of Boron in Dispersion-Strengthened Copper. *Journal of Materials Science*, Vol.27, No.21 (November 1992), pp. 5926-5930, ISSN 0022-2461
- Gessinger, G.H. (1976). Mechanical Alloying of IN-738. *Metallurgical Transactions A*, Vol.7, No.8, (August 1976), pp. 1203-1209, ISSN 0360-2133
- Hirsch, J. & Lücke, K. (1988). Mechanism of Deformation and Development of Rolling Textures in Polycrystalline FCC Metals-I. Description of Rolling Texture Development in Homogeneous CuZn Alloys. *Acta Metallurgica*, Vol.36, No.11, (November 1988), pp. 2863-2882, ISSN 1359-6454
- Humphreys, F.J. & Hatherly, M. (1995). *Recrystallization and Related Annealing Phenomena*, Pergamon, ISBN 0-08-041884-8, Oxford, United Kingdom
- Kim, S.-H. & Lee, D.N. (2001). Recrystallization of Alumina Dispersion Strengthened Copper Strips. *Materials Science and Engineering A*, Vol.313, No.1-2, (August 2001), pp. 24-33, ISSN 0921-5093
- Kim, S.-H. & Lee, D.N. (2002). Annealing Behavior of Alumina Dispersion-Strengthened Copper Strips Rolled Under Different Conditions. *Metallurgical and Materials Transactions A*, Vol.33, No.6 (June 2002), pp. 1605-1616, ISSN 1073-5623
- Klug, R.C.; Krauss, G. & Matlock, D.K. (1996). Recrystallization in Oxide-Dispersion Strengthened Mechanically Alloyed Sheet Steel. *Metallurgical and Materials Transactions A*, Vol.27, No.7, (July 1996), pp. 1945-1960, ISSN 1073-5623
- Kusunoki, K.; Sumino, K.; Kawasaki, Y. & Yamazaki, M. (1990). Effects of the Amount of γ' and Oxide Content on the Secondary Recrystallization Temperature of Nickel-Base Superalloys. *Metallurgical Transactions A*, Vol.21, No.2, (February 1990), pp.547-555, ISSN 0360-2133
- Matthies, S.; Vinel, G.W. & Helming, K. (1987). *Standard Distribution in Texture Analysis*, Akademie-Verlag, ISBN 3-05-500249-0, Berlin, Germany
- Mino, K.; Nakagawa, Y.G. & Ohtomo, A. (1987). Abnormal Grain Growth Behavior of An Oxide Dispersion Strengthened Superalloy. *Metallurgical Transactions A*, Vol.18, No.6, (June 1987), pp. 777-784, ISSN 0360-2133
- Miodownik, M.A.; Martin, J.W. & Little, E.A. (1994). Secondary Recrystallization of Two Oxide Dispersion Strengthened Ferritic Superalloys : MA956 and MA 957. *Materials Science and Technology*, Vol.10, No.2, (February 1994), pp. 102-109, ISSN 0267-0836
- Miodownik, M.A.; Humphreys, A.O. & Martin, J.W. (1995). Growth of Secondary Recrystallized Grains during Zone Annealing of Oxide Dispersion Strengthened Alloys. *Materials Science and Technology*, Vol.11., No.5, (May 1995), pp. 450-454, ISSN 0267-0836
- Nadkarni, A. (1984). Dispersion Strengthened Copper Properties and Applications, In : *High Conductivity Copper and Aluminum Alloys*, E. Ling, P.W. Taubenblat, (Ed.), 77-101, TMS-ASME, Warrendale, PA

- Petrovic, J.J. & Ebert, L.J. (1972). Electron Microscopy Examination of Primary Recrystallization in TD-Nickel. *Metallurgical Transactions*, Vol.3, No.5, (May 1972), pp.1123-1129, ISSN 0360-2133
- Petrovic, J.J. & Ebert, L.J. (1972). Abnormal Grain Growth in TD-Nickel. *Metallurgical Transactions*, Vol.3, No.5, (May 1972), pp.1131-1136, ISSN 0360-2133
- Preston, O. & Grant, N.J. (1961). Dispersion Strengthening of Copper by Internal Oxidation. *Transactions of the Metallurgical Society of AIME*, Vol.221, (February 1961), pp.164-173
- Randle, V. (1993). *The Measurement of Grain Boundary Geometry*, Institute of Physics Publishing, ISBN 0-7503-0235-6, London, United Kingdom
- Simchi, H. & Simchi, A. (2009). Tensile and Fatigue Fracture of Nanometric Alumina Reinforced Copper with Bimodal Grain Size Distribution. *Materials Science and Engineering A*, Vol.507, No.1-2, (May 2009), pp. 200-206, ISSN 0921-5093
- Singer, R.F. & Gessinger, G.H. (1982). The Influence of Hot Working on the Subsequent Recrystallization of a Dispersion Strengthened Superalloy-MA 6000. *Metallurgical Transactions A*, Vol.13, No.8, (August 1982), pp. 1463-1470, ISSN 0360-2133
- Stephens, J.J. & Nix, W.D. (1985). The Effect of Grain Morphology on Longitudinal Creep Properties of INCONEL MA 754 at Elevated Temperature. *Metallurgical Transactions A*, Vol.16, No.7, (July 1985), pp. 1307-1324, ISSN 0360-2133
- Sumino, Y.; Watanabe, H. & Yoshida, N. (2009). The Microstructural Evolution of Precipitate Strengthened Copper Alloys by Varying Temperature Irradiation. *Journal of Nuclear Materials*, Vol.386-388, No.C, (April 2009), pp. 654-657, ISSN 0022-3115
- Young, C.T.; Steele, J.H. & Lytton, J.L. (1973). Characterization of Bicrystals Using Kikuchi Patterns, *Machine Design*, Vol.4, No.9, (September 1973), pp. 2081-2089, ISSN 0024-9114

IntechOpen



Recrystallization

Edited by Prof. Krzysztof Sztwiertnia

ISBN 978-953-51-0122-2

Hard cover, 464 pages

Publisher InTech

Published online 07, March, 2012

Published in print edition March, 2012

Recrystallization shows selected results obtained during the last few years by scientists who work on recrystallization-related issues. These scientists offer their knowledge from the perspective of a range of scientific disciplines, such as geology and metallurgy. The authors emphasize that the progress in this particular field of science is possible today thanks to the coordinated action of many research groups that work in materials science, chemistry, physics, geology, and other sciences. Thus, it is possible to perform a comprehensive analysis of the scientific problem. The analysis starts from the selection of appropriate techniques and methods of characterization. It is then combined with the development of new tools in diagnostics, and it ends with modeling of phenomena.

How to reference

In order to correctly reference this scholarly work, feel free to copy and paste the following:

Su-Hyeon Kim and Dong Nyung Lee (2012). Recrystallization of Dispersion-Strengthened Copper Alloys, Recrystallization, Prof. Krzysztof Sztwiertnia (Ed.), ISBN: 978-953-51-0122-2, InTech, Available from: <http://www.intechopen.com/books/recrystallization/recrystallization-of-dispersion-strengthened-copper-alloys>

INTECH
open science | open minds

InTech Europe

University Campus STeP Ri
Slavka Krautzeka 83/A
51000 Rijeka, Croatia
Phone: +385 (51) 770 447
Fax: +385 (51) 686 166
www.intechopen.com

InTech China

Unit 405, Office Block, Hotel Equatorial Shanghai
No.65, Yan An Road (West), Shanghai, 200040, China
中国上海市延安西路65号上海国际贵都大饭店办公楼405单元
Phone: +86-21-62489820
Fax: +86-21-62489821

© 2012 The Author(s). Licensee IntechOpen. This is an open access article distributed under the terms of the [Creative Commons Attribution 3.0 License](#), which permits unrestricted use, distribution, and reproduction in any medium, provided the original work is properly cited.

IntechOpen

IntechOpen